

The Existence of a Voltage Collapse Solution in the Static-Dynamic Gap

L. Shalalfeh¹ and E. Jonckheere¹

Abstract—Voltage collapse is one of the critical phenomena that threatens the power infrastructure. It manifests itself by a sudden and fast collapse of the system voltage. The simplest bus system—one generator, one line, and one load describing function—reveals a feedback structure, which, depending on the nature of the load, could go in a voltage collapse resembling an “anti van der Pol” behavior. A static-dynamic compromise for the load model is provided by an “impedance” describing function that has the advantage of being derived from experimental data collected in a real grid environment [5]. This reveals, among other things, a noninteger exponent of the frequency requiring a real analytic extension for the model to be usable for a collapsing solution away from the imaginary axis. We investigate whether the voltage collapse is possible to occur at different loads. In the cases where the voltage collapse is likely to occur, we study the interaction between the voltage and frequency during the collapse.

I. INTRODUCTION

Voltage collapse is an intriguing phenomenon from a control perspective. Even though many theoretical “routes” to voltage collapse have already been proposed, it is not entirely clear what is really happening in the complex, large-scale environment of the power grid. It is our contention that voltage collapse is not just a supply-demand imbalance, but is rather a nonlinear phenomenon due to the complicated characteristics of the typical “messy” loads that the generators drive. The early suspicion that load characteristic is somehow the culprit in voltage collapse has led to deeper research on load modeling. Load characteristics, outside the realm of classical circuit theory because of their unusual frequency dependence, have indeed been shown to be related to voltage collapse, but in a context where other phenomena (e.g., tap-changer effects) contribute to the collapse. In this paper, we show that voltage collapse can occur—even with an infinite bus, even with a simple one-generator, one-line, one-load configuration—as a phenomenon emanating from special effects in the aggregated load characteristic. Voltage collapse here is to be understood in a strong sense; namely, because of a hidden feedback effect, as the load voltage decreases the damping of the oscillation increases. We call this phenomenon, the *anti-Van der Pol effect*.

Voltage collapse has been studied in the literature using different methods and using several power system models. The voltage collapse has been explained using static and dynamic analysis. In the static analysis, investigators introduced several measures for the voltage collapse, like existence of power flow solution, singularity of the Jacobian matrix [13], etc. On the other hand, the dynamic analysis

of the voltage collapse was based on studying the dynamic interactions between the components of the power system, like the generator and load dynamics [?], load and tap changer dynamics [12], etc.

It is generally believed that the dynamics of the loads is an important factor in voltage collapse. Several models were introduced to describe the nonlinearity and dynamics of the load. The loads in the power system are modeled either as static or dynamic loads. In static loads, active and reactive powers are represented as possibly non integer powers of the load voltage with exponents n_p, n_q that depend on the load type as shown in Eq. (1),

$$P_L = K_p V_L^{p_v}, \quad Q_L = K_q V_L^{q_v}, \quad (1)$$

where K_p and K_q are constants. Classically, there are three types of static loads: constant power ($p_v = q_v = 0$), constant current ($p_v = q_v = 1$), and constant impedance ($p_v = q_v = 2$).

The static load has been used to study the voltage collapse by looking at the feasibility of the load flow [7], the minimum singular value of the Jacobian matrix [13], and static bifurcations of the load flow equations [11].

The dynamic load model, which was proposed in Hill [8], captures the transient load response to voltage step function. The model represents the power as solution to a nonlinear differential equation. This model has been used to study the voltage collapse in the power system looking at the interactions between the dynamics of the load and the generator or the load and the on-load tap changer as in [12].

In this paper, we use another load model, the Berg model [4], which in our opinion has been overlooked. Probably its most distinguishing feature is that it was derived in a real grid environment, which probably explains, in addition to noninteger exponents n_p and n_q of the load voltage, noninteger exponents of the frequency w , as shown in Eq. (2). Because of this frequency dependence, we refer to those models as “in the static-dynamic gap.” These models lend themselves to describing function “impedance” models, which are easily incorporated in multivariable feedback diagram and amenable to robust multivariable control techniques to reveal the possibility or the impossibility of voltage collapse.

This paper is organized as follows. In Sec. II, the power system model and its components are introduced. The existence of voltage collapse solution will be covered in Sec. III. Then, the possibility of voltage collapse for different loads will be covered in Section IV, and we have the conclusion in Sec. V.

(1) Dept. of Electrical Engineering, Univ. of Southern California, Los Angeles, CA 90089-2563 {shalalfe, jonckhee}@usc.edu

II. POWER SYSTEM MODEL

The power system model consists of one generator source connected to a load (\mathbf{Z}_L) through a transmission admittance (\mathbf{Y}_{Line}), as shown in Fig. 1a. The circuit diagram in Fig. 1a can be redrawn to highlight the feedback structure with the line admittance (\mathbf{Y}_{Line}) in the feedforward transfer function and the load (\mathbf{Z}_L) is the feedback transfer function. This representation will be used through the whole analysis. The feedback model is shown in Fig. 1b.

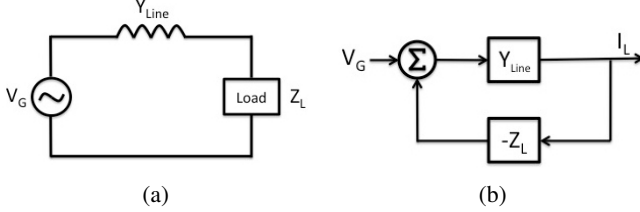


Fig. 1: Power system model: (a) Circuit diagram, (b) Feed-back model

The generator will be modeled using a harmonic oscillator with a resonance frequency $\omega_0 = 377 \text{ rad/s}$. Even though the generator model is a simplified one, it still will give us some insight on how the voltage could collapse. A block diagram of the generator model is shown in Figure 2.

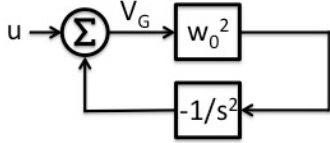


Fig. 2: Block Diagram of the harmonic oscillator

The transmission line will be represented by an inductive admittance (\mathbf{Y}_{Line}), assuming the purely inductive transmission line property can be justified as an approximation, that is, the resistance and the capacitive effects of the transmission line will be neglected. In this paper, will study different types of loads, one by one, to show conditions under which voltage collapse occurs. These models will be explained in details in the next subsection.

A. Static-dynamic gap load modeling

Here, we fill the so-called “static-dynamic” gap by introducing describing function models of such usual loads as reduction furnace, fluorescent lamps, etc. The static model, the (P, V) diagram, is well known and not reviewed here. The popular dynamical model of Hill [8] relies on a differential equation linking the instantaneous active power consumed by the load, the static power, and the voltage magnitude under subharmonic transients.

On the other hand, the Berg model [4] adopted here ignores transients, but runs at the harmonic level and is hence amenable to robust multivariable techniques. In a certain sense, we compromise between static and dynamic, with a purely harmonic model analytically extendable to

TABLE I: Typical values of characteristic-load parameters

Load Type	p_v	p_w	q_v	q_w
Filament lamp	1.6	0	0	0
Fluorescent lamp	1.2	-1.0	3.0	-2.8
Heater	2.00	0	0	0
Induction motor half load (HL)	0.2	1.5	1.6	-0.3
Induction motor full load (FL)	0.1	2.8	0.6	1.8
Reduction furnace	1.9	-0.5	2.1	0
Aluminum plant	1.8	-0.3	2.2	0.6
Regulated aluminum plant	2.4	0.4	1.6	0.7

include slightly damped behavior, and amenable to large scale analysis.

In the Berg model [4], the active power P_L and the reactive power Q_L consumed are noninteger exponent powers of the load voltage amplitude V_L and the frequency w as shown in Eq. (2),

$$P_L = K_p V_L^{p_v} w^{p_w}, \quad Q_L = K_q V_L^{q_v} w^{q_w}, \quad w > 0. \quad (2)$$

In the above, K_p and K_q are constants. The exponents p_v , p_w , q_v , and q_w depend on the specific load. Table I shows the exponents for different loads (from [1, Table 6.1], [4], [5]).

The describing function of the load represents the equivalent gain from the load current \mathbf{I}_L to load voltage \mathbf{V}_L , $\mathbf{Z}_L = \frac{\mathbf{V}_L}{\mathbf{I}_L}$. By multiplying the numerator and denominator by \mathbf{V}_L^* , we get

$$\mathbf{Z}_L = \frac{\mathbf{V}_L \mathbf{V}_L^*}{\mathbf{I}_L \mathbf{V}_L^*} = \frac{V_L^2}{\mathbf{S}_L^*}. \quad (3)$$

The complex power is equal to

$$\mathbf{S}_L = \mathbf{V}_L \mathbf{I}_L^* = P(V_L, w) + jQ(V_L, w). \quad (4)$$

Substituting Eq. (4) in Eq. (3) yields

$$\mathbf{Z}_L = \frac{V_L^2}{P(V_L, w) - jQ(V_L, w)}. \quad (5)$$

The describing function of different power grid loads can be derived by substituting the expression for P , Q of Eq. (2) in the describing function equation (5). The describing function of the load becomes:

$$\mathbf{Z}_L = \frac{1}{K_p V_L^{p_v-2} w^{p_w} - jK_q V_L^{q_v-2} w^{q_w}}, \quad (6)$$

The describing functions of different types of loads are shown in Table II.

B. Berg [4] model versus Hill model [8]

The dynamical, transient-motivated model developed by Hill [8] reads

$$T_p \dot{P}_d + P_d = P_s(V_L) + k_p(V_L) \dot{V}_L$$

where P_d is the slowly time-varying active power consumed by the load and P_s is the steady-state component of the active power. $P_s(V_L)$ is certainly comparable with Model (1), valid in the specific cases of the filament lamp and the heater where the Berg modeling does not reveal frequency

TABLE II: Impedances of various loads

Load Type	Describing Function
Filament lamp	$\frac{1}{K_p V_L^{-0.4} - j K_q V_L^{-2}}$
Fluorescent lamp	$\frac{1}{K_p V_L^{-0.8} w^{-1} - j K_q V_L w^{-2.8}}$
Heater	$\frac{1}{K_p - j K_q V_L^{-2}}$
Induction motor HL	$\frac{1}{K_p V_L^{-1.8} w^{1.5} - j K_q V_L^{-0.4} w^{-0.3}}$
Induction motor FL	$\frac{1}{K_p V_L^{-1.9} w^{2.8} - j K_q V_L^{-1.4} w^{1.8}}$
Reduction furnace	$\frac{1}{K_p V_L^{-0.1} w^{-0.5} - j K_q V_L^{0.1}}$
Aluminum plant	$\frac{1}{K_p V_L^{-0.2} w^{-0.3} - j K_q V_L^{0.2} w^{0.6}}$
Regulated aluminum plant	$\frac{1}{K_p V_L^{0.4} w^{0.4} - j K_q V_L^{-0.4} w^{0.7}}$

dependence. The major difference, however, is that \dot{P}_d and \dot{V}_L are the time derivatives of the *active* power and the voltage *magnitude*, resp., so that any describing function attempt to replace d/dt by jw_{sub} , viz.,

$$P_d(jw_{\text{sub}}, V_L) = \frac{\alpha P_s(V_L) + \beta jw_{\text{sub}} k_p(V_L) V_L}{1 + jw_{\text{sub}} T_p}$$

would entail a subharmonic component w_{sub} , while the Berg model entail the harmonic (line frequency) w .

In a certain sense, the Berg and the Hill models complement each other, both having the similarity of a slow transient followed by recovery to steady-state (compare Berg [4, Fig. 8] with Hill [8, Fig. 1]). The discrepancy is that the Berg model ignores the transient but captures a noninteger power of the frequency component in the steady-state whereas the Hill model captures the transient but ignores the frequency-dependence of the steady-state.

This noninteger exponent in the Berg model is probably due to a nonlinear load aggregation effect in the grid, as the Berg model measured the dependency of the active power on voltage and frequency at the specific load, but in a real Scandinavian island grid. It could be argued that such exponents as $w^{-2.1}$ in the induction motor could be the result of experimental inaccuracies, but such exponents as $w^{0.5}$ in the reduction furnace point to an inescapable reality, which was recently corroborated by [9] as fractional derivatives in transformer models.

III. EXISTENCE OF A VOLTAGE COLLAPSE SOLUTION

Combining the generator model and the power system model, we will have the feedback model that is shown in Fig. 3. The model has a 2×2 feedforward transfer matrix (G). The matrix G is an upper-triangular matrix, which has Y_{Line} and w_0^2 on the diagonal. The feedback transfer matrix (F) is a 2×2 diagonal matrix with $-Z_L$ and $-\frac{1}{s^2}$ on the diagonal.

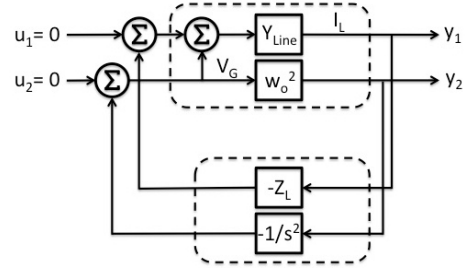


Fig. 3: Block diagram of the power system including the harmonic oscillator

The output ($y = [y1 \ y2]^t$) can be written as function of the input ($u = [u1 \ u2]^t$), as follows:

$$y = (I - GF)^{-1} Gu, \quad (7)$$

where

$$G = \begin{pmatrix} \mathbf{Y}_{\text{Line}} & \mathbf{Y}_{\text{Line}} \\ 0 & w_0^2 \end{pmatrix}, \quad F = \begin{pmatrix} -\mathbf{Z}_L & 0 \\ 0 & -\frac{1}{s^2} \end{pmatrix}.$$

It is important to note that Equation (7) *should not* be interpreted as a Laplace transform equation, but as an equation where $y(jw)$ and $u(jw)$ are “phasors” of the harmonic regime $\cos wt$ in a sense formalized in [3]. We will further extend jw to $s = \sigma + jw$ where s is restricted to a small strip across the imaginary axis, where the analytic extension of the frequency response of the loads is guaranteed to exist, as will be proved in Sec. III-A. Such an extension for stability analysis has been validated in [2].

A. Analyticity

Voltage collapse would mean showing that a purely harmonic solution to feedback equations under some V_L would go to a solution of the form $e^{\sigma t} \cos(wt)$, $\sigma < 0$, when V_L drops below some nominal voltage. There is thus a need to validate the various describing functions for such signals, that is, do an analytical extension to $w - j\sigma$. The nonlinear impedance can clearly be written as $\mathbf{Z}_L = R_L + jX_L$ and it is easily seen that both R_L and X_L are of the form $p(V_L, w)/q(V_L, w)$; some further manipulations allow us to rearrange terms so that both the numerator and the denominator of R_L , X_L involve positive (possibly noninteger) powers of w .

Lemma 1: If $p(V_L, w)$ and $q(V_L, w)$ are real analytic in w around $w_0 = 2\pi \times 60$, and if $q(V_L, w_0) \neq 0$, then $p(V_L, w)/q(V_L, w)$ is real analytic at w_0 .

Proof: Define the function $\text{inv}(x) = 1/x$. It is real analytic at $x \neq 0$. Next, observe that $1/q(V_L, w) = (\text{inv} \circ q)(V_L, w)$. Since the composition of two real analytic functions is real analytic [10, Prop. 1.4.2] (a corollary of the Faà di Bruno formula [10, Sec. 1.3]), it follows that $1/q(V_L, w)$ is real analytic. Finally, $p(V_L, w)/q(V_L, w)$ is real analytic as the product of two real analytic functions having nonempty intersection of their domain of convergence [10, [Prop. 1.1.7]. ■

It remains to show that $p(V_L, w)$ and $q(V_L, w)$ are real analytic. Clearly, it suffices to show that w^r , where $r > 0$

is a noninteger, possibly irrational exponent, is analytic. We simplify the exposition by assuming that $r \in \mathbb{Q}_+$.

Lemma 2: $w^{n/d}$, where $n, d \in \mathbb{N}$ is real analytic around $w \neq 0$.

Proof: Define the power function $\text{power}_r(x) = x^r$. For $n \in \mathbb{N}$, power_n is clearly real analytic. Furthermore, $\text{power}_{1/d}$ is real analytic by the real analytic inverse function theorem [10, Sec. 1.5]. Finally, observe that $w^{n/d} = (\text{power}_{1/d} \circ \text{power}_n \circ 1)(w)$ and the latter is real analytic by the real analytic property of the composition of real analytic functions. ■

B. Voltage collapse condition

The possibility for the power system in Fig. 1(a) to have oscillation is determined by Eq. (7). The power system will have a solution for the output (y) when the input (u) is equal to zero iff the determinant of $(I - GF)$ is equal to zero. The determinant of $(I - GF)$ can be written as

$$|I - GF| = (1 + \mathbf{Z}_L \mathbf{Y}_{\text{Line}}) \left(1 + \frac{w_0^2}{s^2}\right). \quad (8)$$

Theorem 1: Consider the feedback interconnection of Fig. 3. Then, on the one hand, a harmonic solution $\cos(\omega t)$ always exists. On the other hand, a voltage collapsing solution $e^{\sigma t} \cos(\omega t)$ with $\sigma < 0$ exists if and only if

$$1 + \mathbf{Z}_L(V_L, w - j\sigma) \mathbf{Y}_{\text{Line}}(w - j\sigma) = 0,$$

for some $\sigma < 0$.

Proof: In the particular case of one generator, one line, one load, the multivariable diagram of Fig. 3 yields y subject to collapse. By having the input u equal to zero in Eq. 7, existence of solutions is then given by $\det(I - GF) = 0$, which yields $(1 + \mathbf{Z}_L \mathbf{Y}_L) \left(1 + \frac{w_0^2}{s^2}\right) = 0$. From here on, the result should be obvious. ■

Assuming the load describing function is not equal to zero at any voltage (V_L) and frequency (w), the voltage collapse condition can be rewritten as

$$\mathbf{Y}_L(V_L, w - j\sigma) + \mathbf{Y}_{\text{Line}}(w - j\sigma) = 0, \quad (9)$$

where

$$\mathbf{Y}_L = K_p V_L^{p_v - 2} \left(\frac{w - j\sigma}{w_0}\right)^{p_w} - j K_q V_L^{q_v - 2} \left(\frac{w - j\sigma}{w_0}\right)^{q_w} \quad (10)$$

and

$$\mathbf{Y}_{\text{Line}} = \frac{K_{\text{Line}}}{\sigma + jw}, \quad (11)$$

where K_{Line} is equal to $\frac{Z_{\text{Line}}}{L}$. For simplification, we will substitute $\sigma + jw$ by s , and multiply Eq.(9) by s . The voltage collapse condition becomes

$$K_p \left(\frac{-j}{w_0}\right)^{p_w} V_L^{p_v - 2} (s)^{p_w + 1} - j K_q \left(\frac{-j}{w_0}\right)^{q_w} V_L^{q_v - 2} (s)^{q_w + 1} + K_{\text{Line}} = 0. \quad (12)$$

In the simple model of Fig. 3, the absence of “back-action” of the load to the generator results in two solutions only—the purely harmonic one imposed by the generator and the

load-specific $1 + \mathbf{Z}_L \mathbf{Y}_{\text{Line}} = 0$ solution. This architecture does not allow for a smooth transition from one to the other, so that some bifurcation needs to be invoked. But, as shown in Sec. IV, the message of this decoupled model is that the $1 + \mathbf{Z}_L \mathbf{Y}_{\text{Line}} = 0$ solution reveals a behavior of the frequency concomitant with the voltage collapse that has been thus far derived in models where the swing equation of the generator appears to play a role [6]. Here, such behavior is created by the load. It thus appears that the load—properly modeled to include the frequency dependence as in the Berg model—might contribute much more to voltage collapse than has been assumed thus far.

IV. THE POSSIBILITY OF VOLTAGE COLLAPSE AT DIFFERENT LOADS

We will go over different groups of power system loads and identify the possibility of voltage collapse in each case. Firstly, we will go over special loads with $p_v = q_v$ and $p_w = q_w$. Then, we will use practical load models that were derived in [5].

Once we write the load impedance as a function of voltage and frequency, we will assume having an analytic extension of the imaginary axis interval $(j(w_0 - \delta), j(w_0 + \delta))$ in which Berg equations are valid to a neighboring strip comprising this interval and intersecting the right and left-half planes. That means that we will replace (w) by $(w - j\sigma)$ in the equations of the load impedance (\mathbf{Z}_L) and the line admittance (\mathbf{Y}_{Line}). Recall that the damping ratio is $\zeta = -\sigma/w$.

A. Special loads with $p_v = q_v, p_w = q_w$

This group of loads have common voltage/frequency exponents for the active power and the reactive power. Even though these loads are more theoretical than realistic, however, they can help us to derive explicit expressions for the damping ratio (ζ) and frequency (w) as functions of the load voltage. Such solution can give us a bound on the voltage ($p_v = q_v$) and frequency ($p_w = q_w$) exponents of the loads that have a potential to collapse. Also, it can explain how other parameters, like active power coefficient (K_p), reactive power coefficient (K_q), and transmission line coefficient (K_{Line}), could support/mitigate voltage collapse.

By having the coefficients of the active and reactive power equal to each other, Eq. (12) can be rewritten as,

$$s = \sigma + jw = \underbrace{\left(\frac{-k_{\text{Line}}}{\left(\frac{-j}{w_0}\right)^{p_w} (K_p - jK_q)}\right)^{\frac{1}{p_w + 1}}}_{\alpha} V_L^{\underbrace{\frac{2 - p_v}{\beta}}_{\beta}}. \quad (13)$$

The system would go to voltage collapse if the following two conditions are satisfied:

Condition 1: $\Re(\alpha) < 0$ & $\Im(\alpha) > 0$

Proof: Given that the damping ratio (ζ) and frequency w are positive during the voltage collapse, and since V_L^β is a real-valued function, the real and imaginary components of α should be negative and positive, resp. ■

Condition 2: $\beta < 0$

Proof: A necessary condition for voltage collapse is that $|\sigma|$ be inversely proportional to V_L , which is satisfied when the exponent β of V_L is negative. ■

Our goal here is to find the ranges of voltage (p_v) and frequency (p_w) exponents that satisfy both of the conditions above. Using MATLAB, we found the region where Condition 1 is satisfied. We used the following numerical values: $K_p = 1$, $K_q = 0.328$, and $K_{Line} = 1000$. Condition 1 depends only on the frequency exponent (p_w) and it is satisfied when $p_w > 0.202$.

The second condition is satisfied if either ($p_v > 2$ & $p_w > -1$) or ($p_v < 2$ & $p_w < -1$). In Fig. 4, we plot the region where Condition 1 holds in red color and the region where Condition 2 in yellow color. The intersection of these regions (orange color) is the region that has potential for voltage collapse.

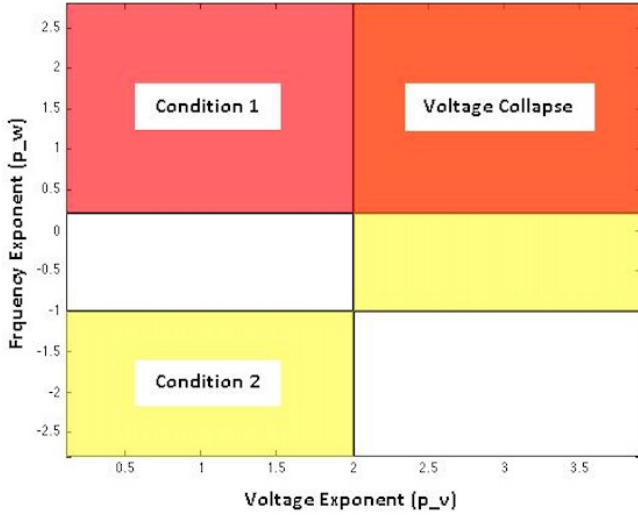


Fig. 4: Voltage collapse region

To confirm the voltage collapse region, we plot σ and the frequency (w) versus the load voltage (V_L) at different load characteristics (p_{v_i}, p_{w_i}) chosen from the voltage collapse region of Fig. 4. We will sweep the voltage from 1 to 0.1. The curves in Fig. 5 for the three loads with exponents pairs ((2.5, 1), (3, 1.5), and (3.5, 2)) are showing increase in the damping ratio as the voltage decrease, which is a voltage collapse scenario.

It is noteworthy that a similar pattern—abrupt decay of voltage concomitant with frequency increase—has already been observed in [6] using an approach that involves the swing equation. Here, we show that a similar behavior can be obtained from the load characteristic only.

B. Berg load models

Now, we will be more interested in applying the voltage collapse condition to the practical loads derived in Section II with load describing functions listed in Table II. Since deriving an expression for the $s = \sigma + jw$ solution is not easy since the voltage collapse condition becomes more

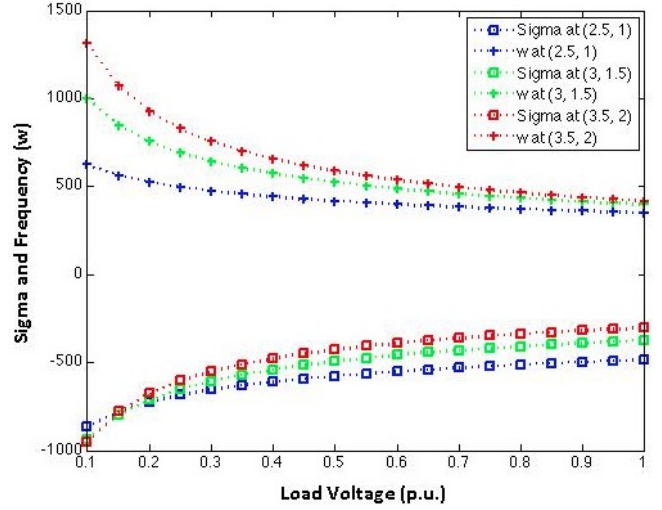


Fig. 5: Sigma (σ) and frequency (w) for different special loads

complicated with multiple non-integer exponents of s , we will use the ‘fsolve’ command in MATLAB to see how the damping ratio (ζ) and the frequency (w) depend on the load voltage (V_L). Based on the results, we can divide the loads into two groups: stable and unstable loads.

1) *Stable loads:* These loads are stable because they are not satisfying the voltage collapse condition. In case of Filament lamp, Heater, and Aluminum plant, the solution of the voltage collapse equation has negative frequency (w) values, which contradicts one of the assumptions (2). The solution of the voltage collapse equation does not exist in case of the Fluorescent lamp and the Reduction furnace.

Induction motors (half/full load) have a solution for the voltage collapse equation; however, the dependence of $|\sigma|$ on the load voltage (V_L) is directly proportional, as shown in Figure 6.

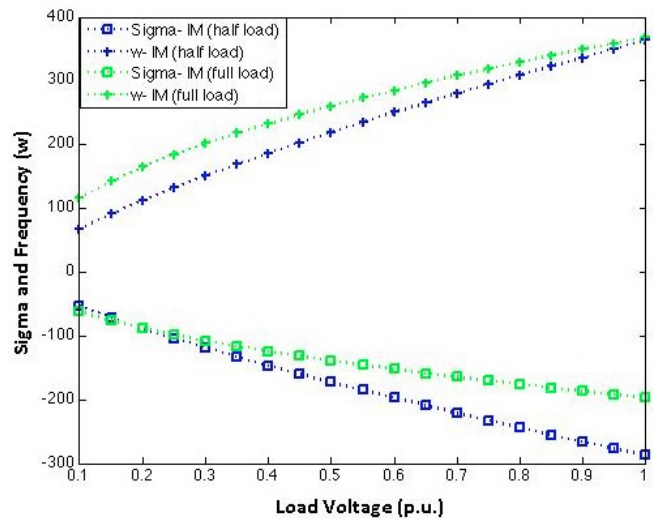


Fig. 6: Sigma (σ) and frequency (w) for induction motor loads (half/full)

2) *Unstable loads:* Regulated Aluminum plant load shows the possibility of having a voltage collapse as shown in Figure 7. This load is Aluminum Plant Load with voltage regulation that is accomplished by a transformer tap changer to maintain constant average load current [4]. Even though the Aluminum plant by itself is a stable load, the equivalent load for the load and the tap changer will make the load vulnerable to voltage collapse.

Again the behavior of Fig. 7 has also been observed in [6] using the swing equation, while here this equation contribution does not appear to play a role.

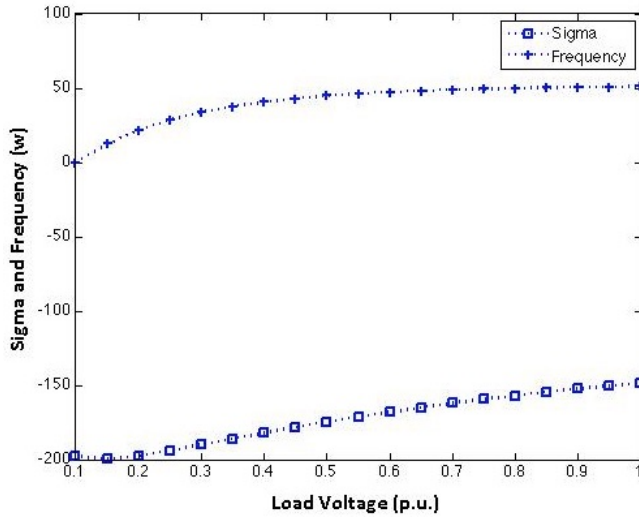


Fig. 7: Sigma (σ) and frequency (ω) for regulated aluminum plant

The transmission line coefficient (K_{Line}), the active power coefficient (K_p), and the reactive power coefficient (K_q) have an impact on the proximity of the power system to voltage collapse. So, we will study how changing these variables could affect the damping ratio (ζ) at nominal load voltage ($V_L = 1$). The closeness of the damping ratio (ζ) to zero at 1 p.u. means that a small bifurcation could throw the voltage along the collapse route and is an indication of higher chance of voltage collapse.

Figs. 8-10 show the dependency of the real part σ on transmission line coefficient, active power and reactive power coefficients. Since the transmission line coefficient (K_{Line}) is equal to $\frac{Z_{base}}{L_{Line}}$ and the maximum power transfer over transmission line is directly proportional to $\frac{1}{L_{Line}}$, the K_{Line} is directly proportional to maximum power transfer. So, Figure 8 indicates that reducing the transmission line capacity could make the system closer to voltage collapse.

The impact of the active and reactive power coefficients on the voltage collapse is shown in Figs. 9-10. The higher these coefficients (K_p and K_q) the higher the load demand, which could make the damping ratio (ζ) have a smaller value at 1 p.u., from where a small disturbance could take the system to voltage collapse.

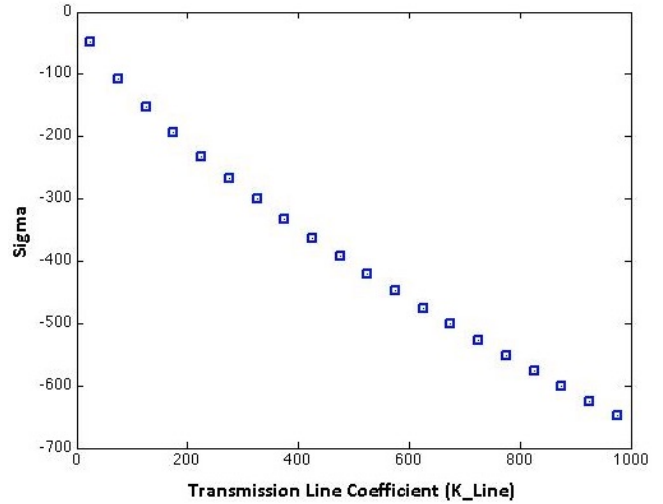


Fig. 8: The relationship between the transmission line coefficient (K_{Line}) and Sigma (σ)

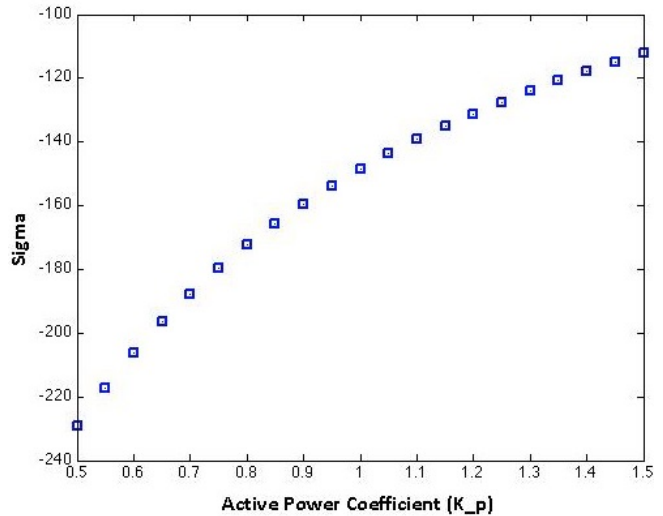


Fig. 9: The relationship between the active power coefficient (K_p) and Sigma (σ)

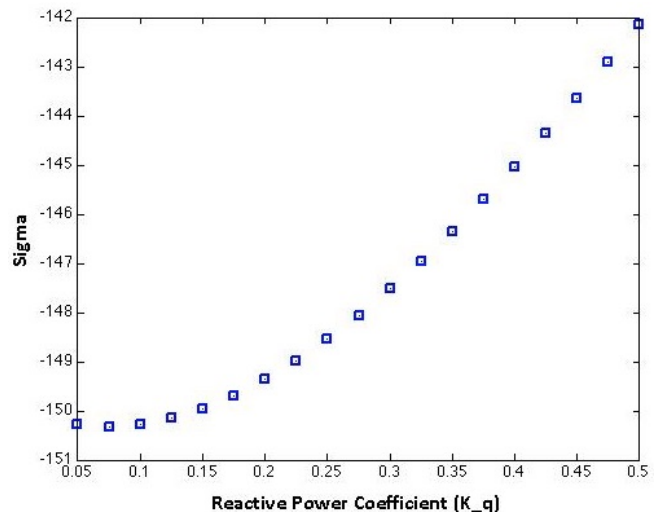


Fig. 10: The relationship between the reactive power coefficient (K_q) and Sigma (σ)

C. Correct initial conditions

Since the results are essentially derived from the load, which, depending on the exponents in the model, would take the system from some initial conditions at 1 p.u. The correct initial conditions should be $\zeta(1\text{p.u.}) = 0$ and $w(1\text{p.u.}) = 2\pi 60$. The curves of Fig. 7 do not quite show the correct initial conditions; however, as shown by Fig. 8, manipulating the transmission line coefficient can bring us close to the correct initial condition $\zeta(1\text{p.u.}) = 0$. The offset of the initial conditions could be created by complicated models extremely sensitive to exponents, themselves difficult to identify.

However, despite this offset in initial conditions most probably created by numerical instability, the trend is correct as corroborated by [6].

V. CONCLUSION

We have shown a hitherto hidden route to voltage collapse. Its main feature is that it involves only a very simple model of the generator together with a model of the load realistically complicated by its strange frequency dependence, indicating that probably load characteristics have been overlooked in the general voltage collapse issue. The culprit seems to be more of an issue of the frequency dependence of the load characteristics rather than its voltage dependence.

Our finding of the possibility of increasing damping together with frequency increase/decrease as the voltage decreases is corroborated by the independent finding of [6], with the difference that our approach places more emphasis on the role of the load in this voltage collapse scenario.

A. Review of main result

As far as the physically realistic frequency-dependent loads as modeled by the Berg paradigm are concerned, they can be classified into two groups:

- Those loads for which the damping ratio ζ decreases as the load voltage decreases (induction motors). For those loads, voltage is stable as, when it tends to decrease, damping is decreasing. This is a Van der Pol-like behavior.
- Those loads that show an increase in damping ζ with decreasing voltage (regulated aluminum plant) together with a frequency disruption. These are the “dangerous” loads, prone to voltage collapse. Indeed, when the load voltage decreases, the damping increases, accelerating the decrease in voltage, in an “anti-Van der Pol” behavior.

Next to the frequency-dependent loads, we also have the frequency-independent loads. Those do not create voltage collapse per the scheme unraveled here.

B. Future work

What still needs further research is the transition from the harmonic regime ($\sigma(1\text{pu}) = 0$) to the regime analyzed here characterized by increased damping under decreasing load voltage. Probably some couplings in Equations (7), (8) should give the key.

As said in Sec. II-B, the Berg model and the Hill model complement each other, on the common foundation of a transient followed by a recovery. It would be beneficial to develop a combined model that would have the unique feature of a harmonic w and a subharmonic w_{sub} frequency dependence.

The issue as to whether the fractional power of the frequency is related to fractional derivatives, as the connection with [9] seems to indicate, is widely open and left for further research.

REFERENCES

- [1] J. Arrillaga and C. P. Arnold. *Computer Analysis of Power Systems*. John Wiley and Sons, Chichester, New York, Brisbane, Toronto, Singapore, 1990.
- [2] D. P. Atherton. *Stability of Nonlinear Systems*. Research Studies Press.
- [3] V. Belevitch. *Classical Network Theory*. Holden-Day, San Francisco, 1968.
- [4] G. J. Berg. System and load behavior following loss of generation—experimental results and evaluation. *Proc. IEE*, 119(10):1483–1486, October 1972.
- [5] G. J. Berg. Power system load representation. *Proc. IEE*, 120(3):344–348, March 1973.
- [6] Claudio A. Canzarez. On bifurcations, voltage collapse and load modeling. *IEEE Transactions on Power Systems*, 10(1), 1995.
- [7] F.D. Galiana. Load flow feasibility and the voltage collapse problem. *IEEE Proceedings of 23rd Conference on Control and Decision*, pages 485–487, December 1984.
- [8] D. J. Hill. Nonlinear dynamic load models with recovery for voltage stability studies. *IEEE Transactions on Power Systems*, 8(1), February 1993.
- [9] A. K. Kamath, J. R. Gandhi, A. S. Bohra, A. V. Goel, D. U. Patil, O. V. Kulkarni, and J. O. Chandle. Modeling of transformer characteristics using fractional order transfer functions. In *IEEE International Conference on Control and Automation*, pages 2123–2128, Christchurch, New Zealand, December 2009.
- [10] S. G. Krantz and H. R. Parks. *A Primer of Real Analytic Functions (Second Edition)*. Birkhäuser Advanced Texts, Boston, Basel, Berlin, 2002.
- [11] H.G. Kwatny, A.K. Pasrija, and L.Y. Bahar. Static bifurcations in electric power networks: Loss of steady-state stability, and voltage collapse. *IEEE Transactions on Circuits and Systems*, CAS-33(10):981–991, October 1986.
- [12] D. Popović, I. A. Hiskens, and D. J. Hill. Investigation of load-tap changer interaction. *Electrical Power & Energy Systems*, 18(2):81–97, 1996.
- [13] A. Tiranuchit and R. J. Thomas. A posturing strategy against voltage instabilities in electric power systems. *IEEE Transactions on Power Systems*, 3(1):87–93, 1988.